A Performance Investigation of Proposed High-Voltage Boost (HVB) DC-DC Converter Fed BLDC Pumping System Using ANFIS Controller

Kshatriya Vamshi Krishna Varma, A. Ramkumar

Abstract*: The economic growth of any country depends on quality and reliable electric power availability to agriculture sector. A simple, efficient and viable power-conditioning structure is introduced for irrigation system with assisted knowledge of advanced intelligent schemes. Among, the classical high-step up converters; a breed of non-isolated high-step-up DC-DC power converter is proposed by utilizing voltage-multiplying modules. The proposed topology can be used as multi-output converter and draw continuous current from single input source in an interleaved approach. The VSI fed brushless DC motor drive is powered by single source High-Voltage Boost (HVB) converter by utilizing solar PV system. The expertise ANFIS prediction scheme is recommended for production of optimum switching states to improve the dynamic response and ameliorate the torque ripples. The versatility of proposed scheme has been developed under variable and/or constant speed conditions by real-time conditions by using computer simulation tool, results are illustrated.

***Index Terms*: Adaptive Neuro-Fuzzy Inference System Controller; BLDC Motor Drive; HVB Converter; Pumping System; Solar PV System**

I. INTRODUCTION

With growing industries and agriculture demand of electric power utility are striving hard to maintain greater power-quality standards in electric power supply [1]-[3]. In order to sustain increased energy demand, bulk power generation capacity is required. The power-utilities are consigned higher priority to large-scale industries; hence agriculture sector and small-scale industries are not being attained the load demand which leads to partial power interruptions, power block-outs, etc. The central power stations are facing several constraints for transforming electrical energy to remote locations and/or hilly areas. Various challenges happen with a simple, low-cost, efficient and reliable ways are greatly influenced by present research towards the renewable energy based pumping applications in agriculture sector.

The solar-PV power generation plays a vital role, becomes prominent over the various RES being utilized in several applications due to noise-free, non-toxic, ample in nature and virtuous. The solar PV energy is integrated to pumping system by employing power conditioning systems [4], in that high-step up DC-DC converter and Voltage-Source Inverter (VSI) plays a major role as a standalone system. The evaluation of DC-DC converter acquires more recognition for attaining high-voltage gain because of the low-voltage coming from solar-PV system, generally in the range of 10V-25V. The outcome of low-voltage SPV is transformed into high-step up voltage up to 200V-500V and integrated to DC-link with effective Maximum-Power Point Tracking (MPPT) algorithm to track the maximum outcome efficiency.

To achieve high-level voltage, formal boost converter requires high duty ratios, which results high dv/dt switch stress. The high-voltage gain can be constrained by presence of parasitic resistive modules, diode-reverse recovery issues and the efficiency is drastically minimized for high duty ratios due to larger current ripples. Generally, couple inductors and high frequency transformers are used to attain high-voltage conversion gain, constraints on transformer design and the leakage currents with more winding turns. In order to develop a high voltage DC-DC converter, the classical DC-DC converters are regular boost converter [5], novel DC-DC converter [22], CUK converter [9], SEPIC converter [10], Modified-SEPIC converter [1], etc. Mohammed Rasheed et al, develops a DC-DC boost converter in [5] for PV applications by using control circuitry for getting desired output voltage. In this circuit, considers input voltage is 23.4V and getting output voltage is nearly 47.3V, the conversion ratio is nearly 1.7%. L. S. Yang & T. J. Liang proposes the novel bidirectional DC-DC converter in [22], consisted of coupled inductors with equal turns operated in a parallel charge and series dis-charge to attain high step-up voltage gain.

In this model, input voltage is considered as 14V and achieve output voltage is nearly 42V; the conversion ratio is nearly 3%. W. Khadmun, W. Subsinghaa presents a new high-voltage gain non-isolated DC-DC boost converter, it transforms 24V input DC voltage to output 130 DC voltage attains the nearly 5.5% conversion ratio. K. V. K Varma et al, proposes the novel M-SEPIC converter utilizing single switch which transforms 112V to 520V with a conversion ratio nearly 5% to 8%.

To obtain the high-voltage gain, a new breed of high-voltage DC-DC converter has been introduced; it can draw energy from two independent DC sources as multi-input converter and/or single source as interleaved approach [11]-[14].

Revised Manuscript Received on December 22, 2018.

Kshatriya Vamshi Krishna Varma, Research Scholar, Department of EEE, Kalasalingam University, Krishnakoil, Tamil nadu, India and Assistant Professor (Head-Training & Placements), Department of EEE, Mahatma Gandhi Institute of Technology, Hyderabad, Telangana, India.

Dr. A. Ramkumar, Associate Professor, Department of EEE, Kalasalingam Academy of Research & Education, Krishnakoil, Tamil nadu, India.

The proposed High-Voltage Boost Converter (HVBC) draws continuous input current from input source with minimum current ripples, low dv/dt switch stress, high efficiency, low EMI compatibility, compact size, and high voltage conversion gain over the formal M-SEPIC converter. The proposed HVBC converter attains a conversion gain of 20%, which transforms the low-level input voltage V_{in}-25V into high-level output voltage V_{out}-500V DC-link. Due to above-mentioned merits, the proposed HVBC converter is good solution to integrate solar PV system into pumping system by using VSI fed BLDC drive system [15]. The imperative merits of BLDC motor over formal motors, like high rugged performance, high efficiency, reliable operation, high torque-weight ratio, low maintenance factor and superior performance characteristics under wide speed regulations [16]-[18].

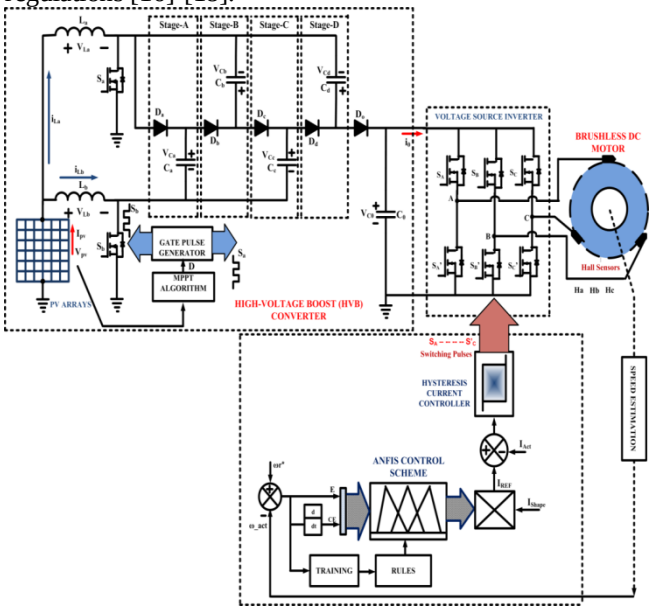

Fig.1: Overall Schematic Diagram of Newly Proposed Single SPV Source based HVB converter fed BLDC Motor Drive

In this paper, a solar PV based HVB DC-DC converter fed BLDC motor drive is proposed by employing Adaptive Neuro-Fuzzy Inference System (ANFIS) controller. The main intension of ANFIS controller is constituted by symbolic path along with intelligent proficiency for prediction of feasible switching states to electronic commutator. It regulates the speed responses under sudden interruptions and regulates the torque ripples over the PI and Fuzzy Controllers. Finally, the well-recognized proposed HVB converter fed BLDC pumping system is more useful for agriculture sector and validated under various control schemes. The evaluation is carried under real-time operating conditions which are constant & variable speed situations verified by Computer Simulation tool and results are illustrated with comparisons.

II. PROPOSED SYSTEM

The newly proposed scheme comprises of a solar-PV arrays, an HVB DC-DC converter, VSI fed BLDC motor drive, and attractive ANFIS controller. The energy in solar-PV feeds the HVB DC-DC converter, controlled by MPPT such that SPV power is optimized then the BLDC to be soft-started. The proposed HVBC draw power from SPV array as interleaved approach and renders the continuous current from SPV array with low ripple current and high-voltage gain. The HVBC transforms energy to BLDC drive through VSI module controlled by optimal switching states. The optimal switching states for VSI module is provoked by current controller with electronic commutator for decoded Hall sensors accorded to rotor position and ANFIS control scheme. The overall schematic diagram of newly proposed single SPV source based HVB DC-DC converter fed BLDC motor drive is shown in Fig.1. The implementation of proposed SPV based HVB converter fed BLDC motor drive with ANFIS controller is described in following sections as;

2.1. Solar PV System

A solar-PV system with the rating of 1.25 KW is not affected by related converter and motor losses; it relies of photo-electric effect to generate the electricity. In the dark regions of the PV cell is akin of regular diode, when the sun-light is more than energy-gap of semiconductor which provides the electrons become free and prevail current flows via external circuitry. As PV cell has low voltage and high fragile formed as arrays and enclosed with a metallic box. Based on required power-levels, the PV cells are interconnected either parallel and/or series to form as array. The mathematical model of PV cell is illustrated in Fig.2. The outcome of PV cell resulted as physical attraction which is related as I_{sv}, I_{phv}, R_{sv}, from the temperature/irradiance levels.

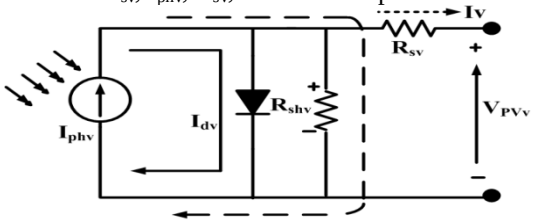

Fig.2: Mathematical model of SPV System

$$Iv = I_{phv} - (I_{sv}\left[\exp q\,\frac{(V_{PVv}+R_{sv}Iv}{NKT}\right] - 1) - \left[\frac{V_{PVv}+R_{sv}Iv}{R_{shv}}\right] \quad (1)$$

The Eqn.1 illustrates the current equation I_v of single PV cell;

Where, I_{phv} represents the Photovoltaic current in amps (A)
I_{sv} represents the Diode's reverse saturation current in amps (A)
K represents the Boltzmann's constant value
N represents the Ideality index factor of diode
q represents the Electron charge
R_{shv} represents the Shunt resistance of PV cell in ohms (Ω)
R_{sv} represents the Series resistance of PV cell in ohms (Ω)
T represents the Junction wise temperature
V_{PVv} represents the Terminal voltage of the diode in volts (V)

A. Proposed HVB DC-DC Converter

The proposed DC-DC converter is influenced from a Dickson Charge pump methodology [20] by utilizing Voltage-Multiplying (VM) circuitry. The diode-capacitor voltage multiplier modules are integrated between the two boost-stages at source level. These VM modules are used to boost the output voltage to acquire high voltage gain, it depends on number of VM modules and the duty-cycles of front-end boost stages. For better-known and simplicity, here considered four-multiplier modules are operated for attaining high voltage gain.

For normal operation, some over-lapping time is defined when dual switches are conducted and other switches should be conducted at any time sequence (see Fig.3). The proposed HVB converter has three working modes, can operate at small duty cycles and no over-lap sequence in between the conduction of respective switches. The proposed HVB converter comprises of single PV source, and dual inductors L_a, L_b, and two MOSFET switches are S_a, S_b. Here considered four VM stages, consisted of four capacitors and diodes such as C_a, C_b, C_c, C_d, and D_a, D_b, D_c, D_d as voltage multiplying circuitry and load is integrated through load capacitor C_0 and diode D_0. The schematic diagram of proposed HVB DC-DC converter is illustrated in Fig.3. The operating modes are illustrated in Fig.4.

Mode-I

In this mode, both the switches S_a, and S_b, are conducted. The dual inductors L_a, and L_b are charged from input source V_{in}. The current in both inductors i_{La} and i_{Lb} raised linearly and the diodes in voltage multiplier module D_a, D_b, D_c, D_d are reverse-biased and under non-conduction as shown in Fig.4(a). The capacitors in VM-module remains un-changed and the load diode D_0 is reverse-biased, thus the load is supported by output capacitor C_0. The energy in C_0 capacitor is delivered to load and maintains load voltage as constant.

Mode-II

In this mode, the switch S_a is non-conducted and S_b, is conducted. The diodes D_a, D_c are forward biased in VM-module. The current flow in inductor L_a is i_{La} and charging the C_a, C_c capacitors and discharging the C_b, C_d, capacitors in VM module. If the number of VM-module is in odd, then the output diode D_0 is in reverse-biased and the load is supported by output capacitor C_0 as shown in Fig.4(b). Moreover, the number of VM-module stage is even, the output diode should be forward bias charges the output capacitor C_0 and providing energy to load. In this case, here considered four VM-stages, the output diode is in forward-bias condition and the energy from main source and VM-capacitors is delivered to load and maintains load voltage as constant.

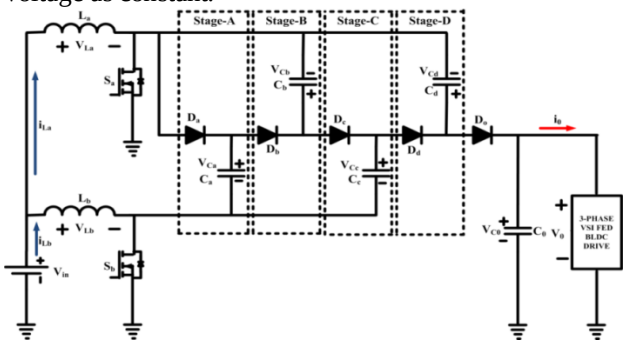

Fig.3: Schematic Diagram of Proposed HVB DC-DC Converter

Mode-III

In this mode, the switch S_a is conducted and S_b is non-conducted. The diodes D_b, D_d are forward biased in VM-module. The current flow in inductor L_b is i_{Lb} and charging the C_b, C_d capacitors and discharging the C_a, C_c, capacitors in VM module. If the number of VM-module is in odd, then the output diode D_0 is in forward-biased charging the output capacitor C_0 and providing energy to load as shown in Fig.4(c). Moreover, the number of VM-module stage is even, the output diode should be reverse bias and the load is supported by output capacitor C_0. In this case, here considered four VM-stages, the output diode is in reverse-bias and the energy in output-capacitor is delivered to load and maintains load voltage as constant.

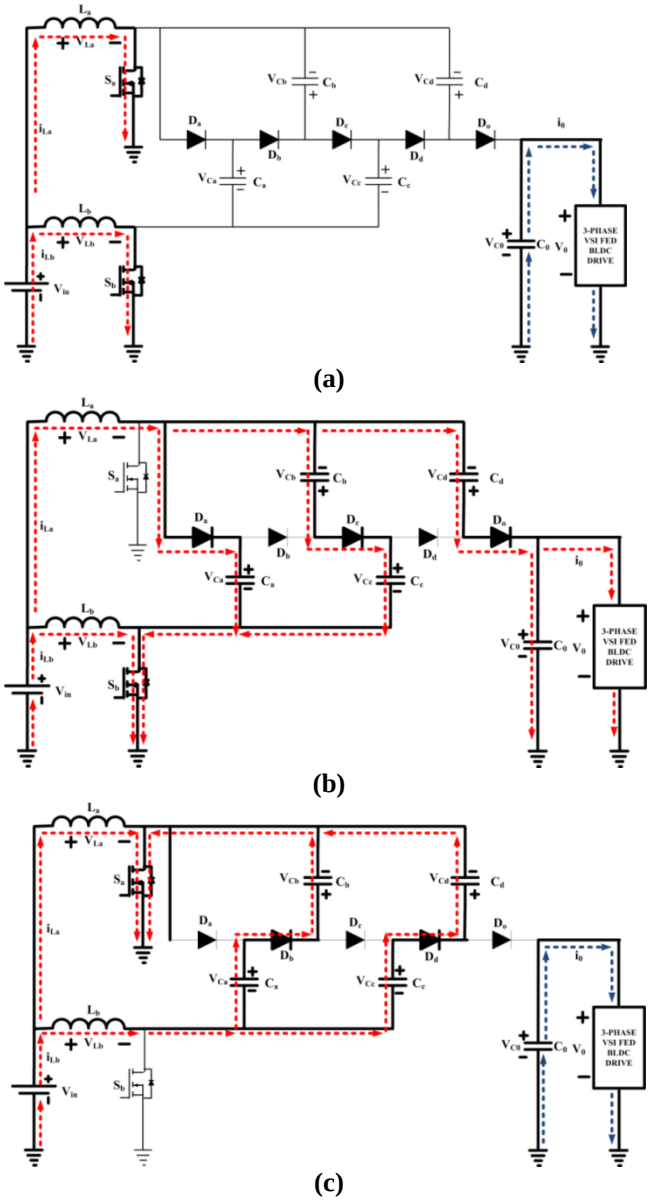

Fig.4: Operating Modes of Proposed HVB DC-DC Converter (a) Mode-I, (b) Mode-II, (c) Mode-III

It can be seen from that, the converter utilizing single DC source and identical duty ratios. When the VM-module is in odd numbered, then the boost-stages consisted of same average inductor currents and otherwise the average current of inductor L_a is greater than inductor L_b. as clearly observed in below Fig.4. When the VM-module is in odd numbered, the average current flows in switch S_b is greater than switch S_a, when VM-module is in even numbered the average current flows in switch S_a is greater than switch S_b. In switch average currents have some small spikes are observed, when the VM-module is in odd numbered the i_{sa} have some spikes and VM-module is in even numbered the spikes are observed in current i_{sb}.

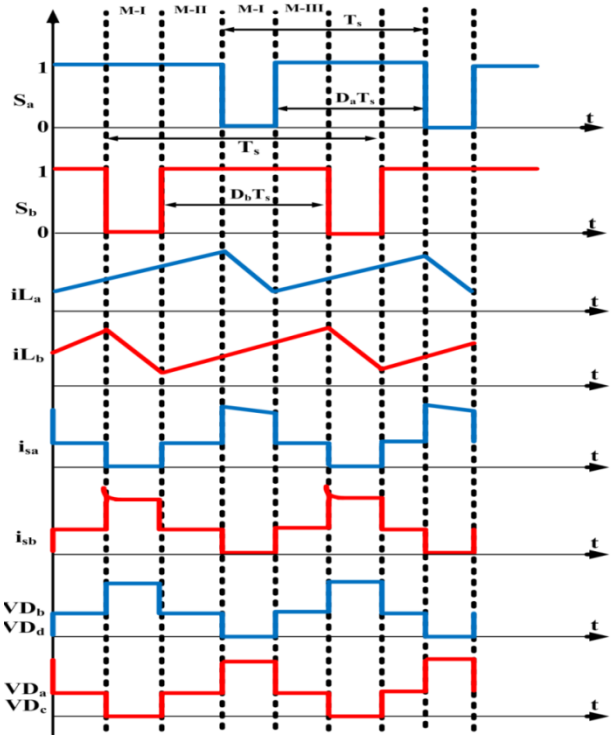

Fig.5: Typical Waveforms for Operating Modes of HVB DC-DC Converter

The presence of spikes in switch current is occurred due to voltage-unbalance between the VM-module capacitors. The switch and diode currents for this converter is operated with four VM-modules, the spikes in i_{sb} is occurred during operating Mode-II. The voltage stress on diodes are totally depends on voltages at capacitor it is interfaced between two VM-module capacitors and is seen in operating mode-II. When switch S_a is non-conduction state and S_b is in conduction state, the diode D_a, D_c are forward bias and other diodes are in blocking mode. Consequently, when switch S_b is in conduction state and S_a is in non-conduction state, the diode D_b, D_d are forward bias and other diodes are in blocking mode as seen in operating mode-III. Moreover, in Mode-III the output diode D_o is conducted, when the VM-module is in odd numbered and conducted in Mode-II when VM-module is in even numbered. The typical waveform of HVB converter under different operating modes is illustrated in Fig.5. The energy is transferred continuously from SPV source to output BLDC drive by charging and/or discharging the VM-module capacitors. For a converter with four working VM-modules, the voltage gain can be established from the volt-sec balance principle of boost inductors. For L_a,

$$V_{La} = 0 \tag{2}$$

Therefore, from Fig.3 (b), it can be observed the voltage across capacitors can be written based on higher boost switching voltage as

$$V_{ca} = V_{cc} - V_{cb} = V_0 - V_{cd} = \frac{V_{in}}{(1-d_a)} \tag{3}$$

Where, d_1 is the duty-cycle of switch S_a. Similarly, from the vol-sec balance principle of lower boost inductor L_b, can write the voltage across capacitors under the lower-boost switching voltage as

$$V_{cb} - V_{ca} = V_{cd} - V_{cc} = \frac{V_{in}}{(1-d_2)} \tag{4}$$

Where, d_2 is the duty-cycle of switch S_b. From (3) and (4), the capacitor voltage for proposed HVBC topology with four VM-modules can be derived as,

$$V_{ca} = \frac{V_{in}}{(1-d_a)}$$

$$V_{cb} = \frac{V_{in}}{(1-d_a)} + \frac{V_{in}}{(1-d_b)}$$

$$V_{cc} = \frac{2V_{in}}{(1-d_a)} + \frac{V_{in}}{(1-d_b)}$$

$$V_{cd} = \frac{2V_{in}}{(1-d_a)} + \frac{2V_{in}}{(1-d_b)} \tag{5}$$

The derived output voltage from (3), which is given by

$$V_0 = V_{cd} + \frac{V_{in}}{(1-d_a)} = \frac{3V_{in}}{(1-d_a)} + \frac{2V_{in}}{(1-d_b)} \tag{6}$$

Similarly, it can be executed with 'N' number of VM-modules.

B. BLDC Motor Drive

A regular VSI topology is utilized to operate the BLDC through electronic commutation process and achieves the feasible operation of pumping system. An electronic commutation activity is pre-requisite for controlling the currents passing through BLDC windings in a specified approach by using decoding circuitry. It should be located symmetrically at DC current component which mid-point of each-operating phase voltage for an angle of 120°. For production of six-switching sequences based on outcomes of hall sensing elements such as H_a, H_b, H_c, and these signals are furnished by pre-defined encoder circuit render to rotor position. A specific interaction of Hall-signals is required for accurate range of rotor angle at the interval of 60°.

Table 1: Switching States for BLDC Drive

Switching Angles	Switch Sequences	Hall Sensors			Conducted Switches		Direction of Phase Current		
		HA	HB	HC			A	B	C
0°~60°	Sa	1	0	0	S_A	S'_B	+ve	-ve	0
60°~120°	Sb	1	1	0	S_A	S'_C	+ve	0	-ve
120°~180°	Sc	0	1	0	S_B	S'_C	0	+ve	-ve
180°~240°	Sd	0	1	1	S_B	S'_A	-ve	+ve	0
240°~300°	Se	0	0	1	S_C	S'_A	-ve	0	+ve
300°~360°	Sf	1	0	1	S_C	S'_B	0	-ve	+ve

The Hall sensors generates the rotor-position to controller, the controller decides the switching angles 0°~60° as a sequence of Sa conducting the switches S_A and S'_B to provide the positive A-phase current to the BLDC drive. Similarly, the controller decides the switching angles 300°~360° as a sequence of Sf conducting the switches S_C and S'_B to provide the positive C-phase current to the BLDC drive. The six switching sequences are instigated for estimating rotor-position as illustrated in Table.1. It is highly recognized, because dual switches are conducted at a time to form 120° switching operation and reduces the conduction losses when operated in 180°. However, the electronic commutation process provides the fundamental switching frequency of the VSI module, for associated switching losses with greater switching frequency based sequences are eliminated.

C. Adaptive Neuro-Fuzzy Inference System (ANFIS) Controller

Various advanced intelligent control objectives are predominantly used in many applications, in that ANFIS control scheme has been recognized because attaining improved performance over PI and Fuzzy controllers [19]. The outstanding characteristics of intelligent controller are comprised as symbolic notation of inference path along with proficiency knowledge. It is pre-requisite for feasible appearance of BLDC motor drive in a SPV pumping application. The best preferable controller for this system is ANFIS, which regulates error quantities in on-going current predominantly minimizes the ripples in electromagnetic torque and enhancing the stability index. It is the vital approach for respective work and yields the switching states to VSI to control the speed of BLDC drive. In ANFIS controller, the proficiency knowledge is achieved from supervised learning methodology by adopting back-propagation algorithm and/or hybrid learning method [20].

The ANFIS controller has incredible capability to achieve optimal membership functions for clustering and deducting for getting stable response within minimum epochs. The main principle of ANFIS structure at initial stage is, it furnishes the test based rules and membership functions which are reorganized as feasible rules and membership functions by using supervised training methodology. If the system doesn't accomplishes the pre-specified error value, the second stage of training is initiated, based on that proficiency knowledge system furnishes the supplement FIS structure with respect to change in error & error sequences. The outcome of ANFIS controller is used as reference signals to generate the switching states to VSI for driving the BLDC motor drive. It can enhance the over-all performance and maximizing the stability index, reducing the electromagnetic torque ripples, smooth function, low noise, good speed regulation, etc. The membership function of ANFIS controller is comprised as error (e) and change in error (Δe) sequences are illustrated in Fig.6.

$$e(s) = \omega^*_{ref} - \omega_{act} \quad (7)$$

$$\Delta e(s) = e(s) - e(s-1) \quad (8)$$

Where, $\boldsymbol{\omega^*_{ref}}$ is reference speed and $\boldsymbol{\omega_{act}}$ is actual speed of BLDC drive, e(s) is speed error value and $\Delta \boldsymbol{e}(\boldsymbol{s})$ is change in error value of speed.

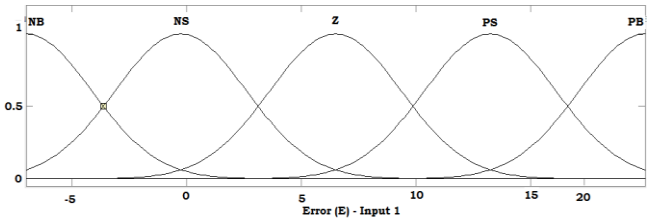

(a)

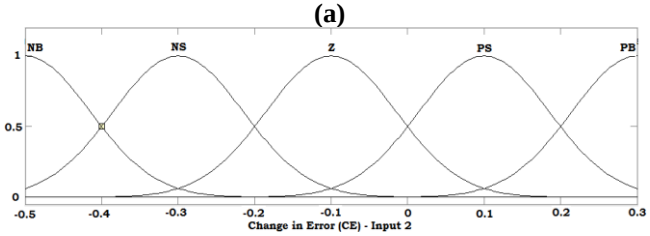

(b)

Fig.6: Membership Functions of ANFIS Controller (a) Error e(s), (b) Change in Error Δe(s)

Several membership functions are EZ-Zero Error; PS-Positive Small; PB-Positive Big and NS-Negative Small and NB-Negative Big value respectively. Several rules of the ANFIS structure are illustrated as below in Table.2. The flowchart of the ANFIS Controller is illustrated in Fig.7.

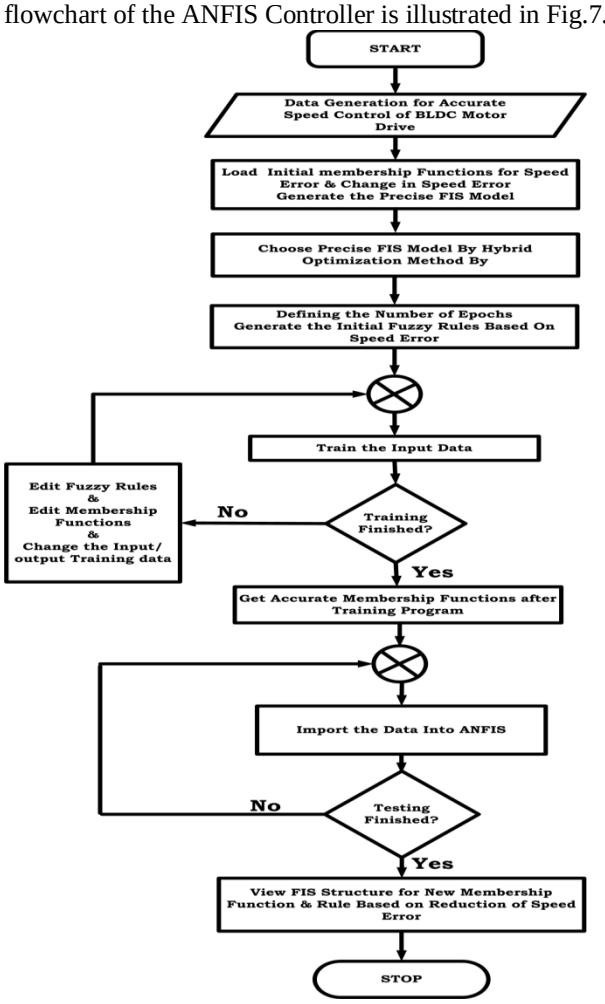

Fig.7: Flowchart of ANFIS Controller

Table 2: Rules for ANFIS Structure

e(s) / $\Delta e(s)$	NB	NS	EZ	PS	PB
NB	R1	R 2	R 3	R 4	R 5
NS	R 6	R 7	R 8	R 9	R 10
Z	R 11	R 12	R 13	R 14	R 15
PS	R 16	R 17	R 18	R 19	R 20
PB	R 21	R 22	R 23	R 24	R 25

III. MATLAB/SIMULINK RESULTS & DISCUSSION

The Matlab/Simulink modeling of proposed system is carried under the both fixed and variable speed conditions, which are operated based on certain specifications, are illustrated in Table.3 at Appendix. The performance of BLDC drive is critically evaluated based on several control functions under constant-speed drive and variable speed conditions as described in below case studies.

A. Evaluation of Several Controllers in a Proposed HVB Converter Fed BLDC Drive under Constant Speed Condition

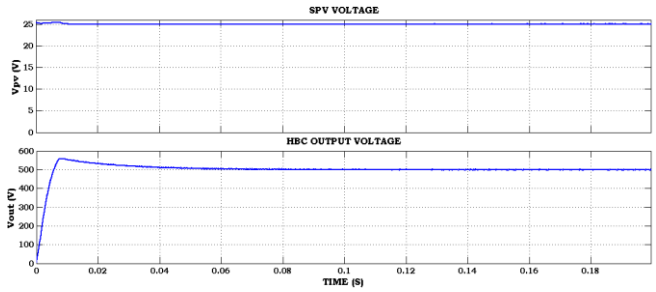

Fig.8: PV Input Voltage & HVB Converter Output Voltage

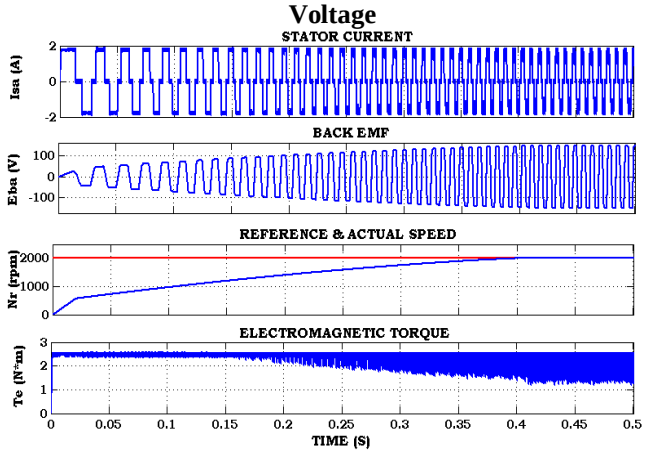

Fig.9: Performance of BLDC Drive under Constant Speed Condition by using PI Controller

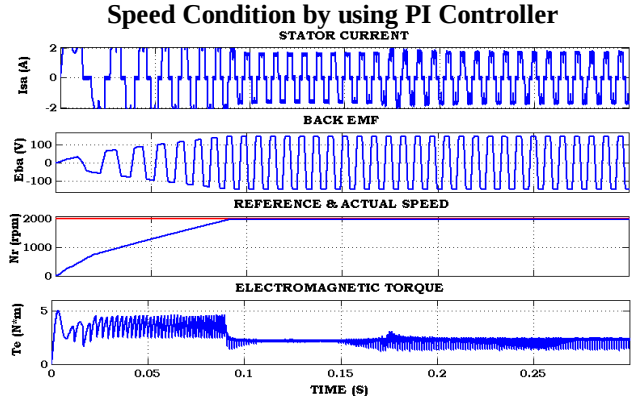

Fig.10: Performance of BLDC Drive under Constant Speed Condition by using Fuzzy Controller

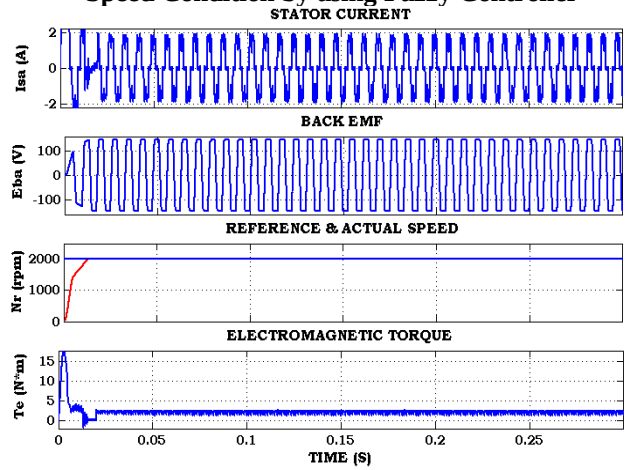

Fig.11: Performance of BLDC Drive under Constant Speed Condition by using Proposed ANFIS Controller

The simulation outcomes of several controllers in a proposed BLDC driven solar-PV system under constant speed condition are clearly evaluated. In that, Fig.8 shows the Input PV voltage and HVBC output voltage. The input voltage is getting 25V from solar-PV array and that voltage is step-up to high-voltage by interfacing proposed HVB DC-DC converter, attains 500V rated voltage to drive the BLDC for pumping application. The performance of BLDC drive under constant speed condition by using PI & Fuzzy, proposed ANFIS controller is evaluated by simulation outcomes as depicted in above Fig.9, Fig.10, Fig.11, respectively. In that, (a) Stator Currents, (b) Back EMFs, (c) Reference & Actual Rotor Speeds, (d) Electro-magnetic Torque, of respective controller. The performance analysis of BLDC motor drive under steady state condition, the motor develops the rated torque at rated speed condition. Due to electronic commutator, the BLDC motor provokes the pulsated electromagnetic torque, makes the mal-function of BLDC motor drive. The performance evaluation of BLDC drive under several controllers under constant speed situations (2000rpm), PI controller attains the rated speed at 0.41 sec and Fuzzy, ANFIS controller attains rated speed at 0.09 sec and 0.015 sec.

At starting condition, electromagnetic torque is very high and requires nearly 20 N-m and when motor in running condition the electromagnetic torque is stabled at 2 N-m due to speed reaches the rated speed at 0.1 sec. The current drawn by the BLDC motor is non-sinusoidal because of VSI; the motor consumes the rated stator current as 1.8A from DC-link. The back EMF of BLDC motor is trapezoidal shape due to 120^{o} mode operation, the rated back-EMF is 110V. Due to demagnetizing currents the electromagnetic torque have some ripples which violates the performance of BLDC motor in running condition which affects the bearings of mechanical system. The magnetizing and de-magnetizing currents are controlled by ANFIS controller which minimizes the ripples in electromagnetic torque and maintains smooth flow of BLDC motor which decreases the noise and better working of bearings. These torque ripples are measured based on differentiation of upper & lower limitations of torque-value under steady-state condition of BLDC motor drive. The torque ripples also reduced with respect to possible control objective, while using PI controller torque ripples factor is 9.48%, Fuzzy controller 11.29% and ANFIS controller 13.42% is decreased. While using PI and Fuzzy controllers have high torque ripples which are eradicated by attractive ANFIS controller.

B. Evaluation of Several Controllers in a Proposed HVB Converter Fed BLDC Drive under Variable Speed Condition

The simulation outcomes of several controllers in a proposed BLDC driven solar-PV system under variable speed condition are clearly evaluated. The performance of BLDC drive under variable speed condition by using PI & Fuzzy, proposed ANFIS controller is evaluated by simulation outcomes as depicted in above Fig.12, Fig.13, Fig.14, respectively. In that, (a) Stator Currents, (b) Back EMFs, (c) Reference & Actual Rotor Speeds, (e) Electro-magnetic Torque, of respective controller. The speed is varied with respect to time such as, at time (t) 0 sec speed (N) is 1500 rpm, at time (t) 0.

15 sec speed (N) is varied to 1500 rpm to 2000 rpm, at time (t) 0.25 sec speed (N) is varied to 2000 rpm to 1400 rpm, at time (t) 0.35 sec speed (N) is varied to 1400 rpm to 2200 rpm, at time (t) 0.45 sec speed (N) is varied to 2200 rpm to 2000 rpm, respectively as maintained as constant. The performance evaluation of BLDC drive under several controllers under variable speed situations (1400 rpm to 2200 rpm), PI controller attains the rated speed at 0.25 sec and Fuzzy, ANFIS controller attains rated speed at 0.06 sec and 0.005 sec. The current drawn by the BLDC motor is non-sinusoidal because of VSI; the motor consumes the rated stator current as 1.8A from DC-link, due to variable speed condition the stator current is slightly affected and maintained as constant. The back EMF of BLDC motor is trapezoidal shape due to 120^{o} mode operation, the rated back-EMF is varied with respect to speed of motor as 100V to 120V.

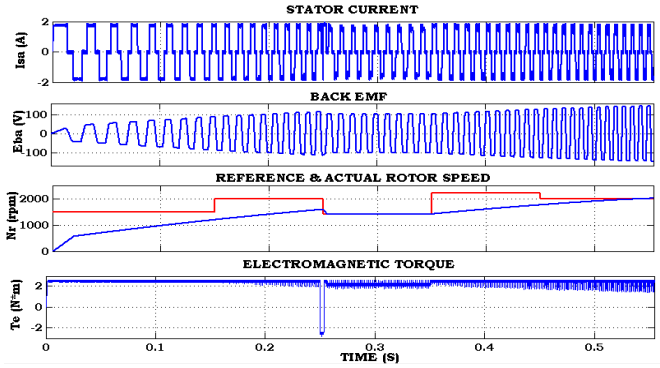

Fig.12: Performance of BLDC Drive under Variable Speed Condition by using PI Controller

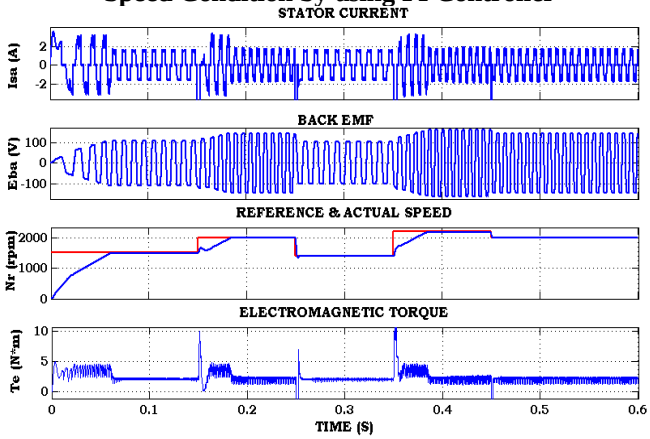

Fig.13: Performance of BLDC Drive under Variable Speed Condition by using Fuzzy Controller

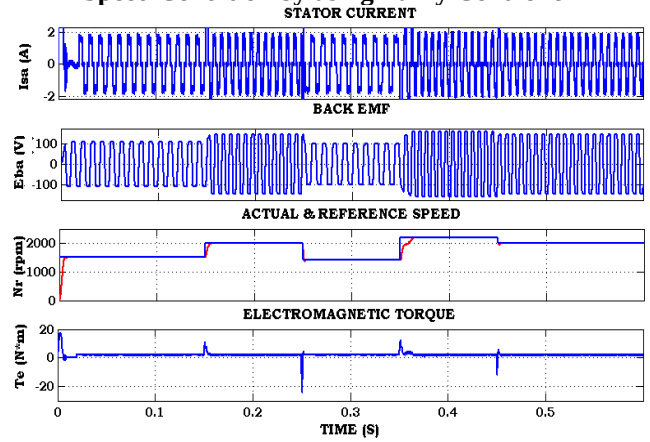

Fig.14: Performance of BLDC Drive under Variable Speed Condition by using Proposed ANFIS Controller

Due to demagnetizing currents the electromagnetic torque have some ripples which violates the performance of BLDC motor in running condition which affects the bearings of mechanical system. The magnetizing and de-magnetizing currents are controlled by ANFIS controller which minimizes the ripples in electromagnetic torque and maintains smooth flow of BLDC motor which decreases the noise and better working of bearings. These torque ripples are measured based on differentiation of upper & lower limitations of torque-value under steady-state condition of BLDC motor drive.

At starting the torque is very high and increased to nearly 20 N-m, in running condition the electromagnetic torque is slightly changed with respect to variable speed condition such as 20 N-m to -20 N-m, getting some small spikes at sudden speed regions and within a relative time which reaches the rated torque. The torque ripples are produced due to electronic commutation unit; these torque pulsations are affecting the motor performance and possible eradication by utilizing proposed ANFIS controller. The torque ripples also reduced with respect to pertained control objective, while using PI controller torque ripples factor is 7.98%, Fuzzy controller 9.28% and ANFIS controller 12.14% is decreased. While using PI and Fuzzy controllers have high torque ripples which are eradicated by attractive ANFIS controller. The performance of proposed BLDC motor drive under several controllers as fixed or variable reference speed condition is clearly illustrated in below Table.4. The Graphical view of Settling time of speed (T_s) in sec and %Torque ripple reduction (T_e) in several controllers under constant & variable speed conditions as illustrated in Fig.15.

Table 4: Comparison of Settling Time & Torque Ripple Reduction in a BLDC Drive System Controlled by Several Controllers under Fixed/Variable Speed Conditions

Parameters	Under Fixed Speed Condition		Under Variable Speed Condition	
	Settling Time of Speed (T_s)	Torque Ripple Reduction (T_e)	Settling Time of Speed (T_s)	Torque Ripple Reduction (T_e)
PI Controller	0.41 sec	9.48%	0.25 sec	7.98%
Fuzzy Controller	0.09 sec	11.29%	0.06 sec	9.28%
ANFIS Controller	0.015 sec	13.42%	0.005 sec	12.14%

The proposed converter utilizes only single source for powering the BLDC drive with the help of HVB converter. The proposed control schemes generates the precise and error free value of reference magnitude for better regulation of BLDC motor speeds and torque ripple minimization. The proposed HVB converter has high step-up conversion ratio over the formal DC-DC converters and more suitable for water-pumping applications. Several converter topologies are studied and compared with respect to voltage gain factor as clearly illustrated in

Table.5, in that proposed HVB DC-DC converter has high step-up voltage gain function and more advantages over the formal converter topologies. The Graphical view of output voltage gains on various formal & proposed DC-DC converter are depicted in Fig.16.

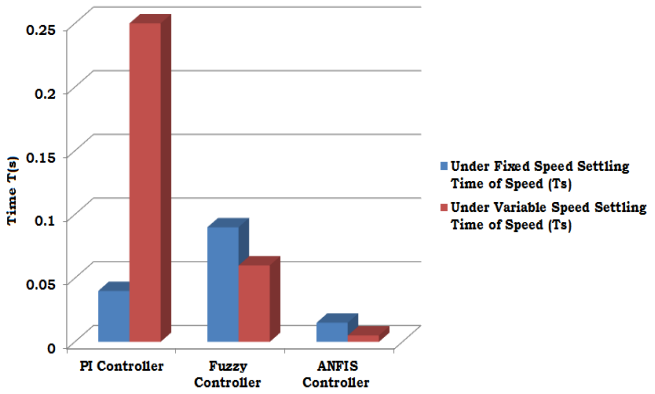

(a) Settling Time of Speed (T_s) in sec

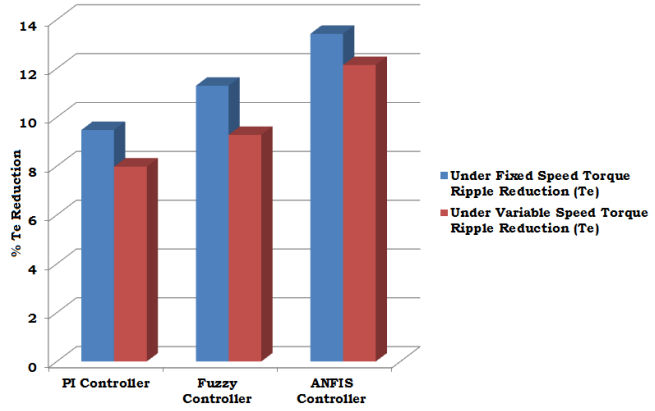

(b) %Torque Ripples Reduction (T_e)

Fig.15: Graphical View of Settling time of speed (T_s) in sec and %Torque ripple reduction (T_e)

Table 5: Comparison of Several Converter Topologies

S.No	Converter Type	Voltage Gain Factor
01	Regular Boost Converter [5]	1.7%
02	Novel DC-DC Converter [22]	3%
03	High-Voltage Boost Converter [8]	5.5%
04	M-SEPIC Converter [1]	5% to 8%
05	Proposed HVB DC-DC Converter	18 to 20%

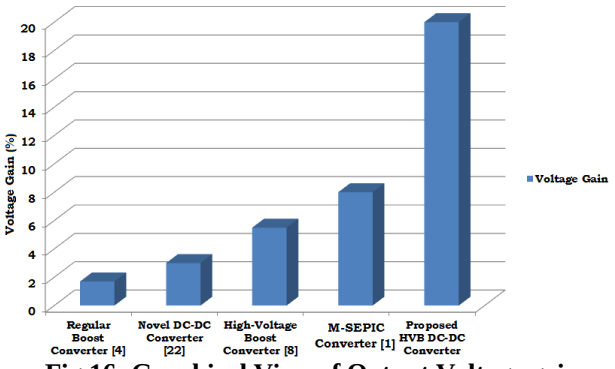

Fig.16: Graphical View of Output Voltage gain on various Formal & Proposed DC-DC Converters

IV. CONCLUSION

In this paper, a new breed of high-voltage boost converter with dual boost stages at input with single source has been proposed for SPV integrated BLDC driven pumping system with various intelligent controllers. The proposed HVBC topology is designed with single source integrated as interleaved approach for getting high-voltage gain by utilizing diode-capacitor voltage multiplier modules. The performance characteristic of proposed system has been evaluated under constant and variable speed situations by using Computer simulation tool. The proposed HVBC topology attains greater voltage under the non-presence of any couple inductors, high voltage gain, low dv/dt switch stress, high efficiency, are the key factors over the classical boost converters. The proposed ANFIS controller regulates the torque ripples and requires less time for attaining steady-state response, enhances the over-all stability index of BLDC drive under speed variations over the PI and Fuzzy controllers. The future recommendation is carried enhancement of BLDC performance under dynamic condition powered by utility grid system.

APPENDIX

Table 3: Operating Specifications

S.No	Parameters	Values
01	PV Input Voltage	25V
02	PV Output Power	1.25KW
03	DC-Link Voltage	500 V
04	Switching Frequency	100KHz
05	Inductors	L_a=100µH; L_b=100µH;
06	Capacitors	C_a=C_b=C_c=C_d=20µF, C_0-22µF
07	Rated Power of BLDC Motor	1 KW
08	Variable Speeds	1400 rpm to 2200 rpm

ACKNOWLEDGMENT

The authors were very special thanks to management of Mahatma Gandhi Institute of Technology (Affliated to JNTUH), Hyderabad, Telangana, India and Kalasalingam Academy of Research & Education, Krishnakoil, Tamil nadu, India for supporting this work.

REFERENCES

1. Vimal Chand Sontake, Vilas R. Kalamkar, "Solar photovoltaic water pumping system - A comprehensive review", *Renewable and Sustainable Energy Reviews*, vol. 59, pp. 1038-1067, June 2016.
2. Mapurunga Caracas, J.V., Carvalho Farias, G.D., Moreira Teixeira, L.F., et al, 'Implementation of a high-efficiency, high-lifetime, and low-cost converter for an autonomous photovoltaic water pumping system', IEEE Trans. Ind. Appl., 2014, 50, (1), pp. 631–641
3. Kim, K.-T., Kwon, J.-M., Kwon, B.-H.: 'Parallel operation of photovoltaic power conditioning system modules for large-scale photovoltaic power generation', IET Power Electron., 2014, 7, (2), pp. 406–417

4. R. Kumar, B. Singh, "BLDC motor driven solar PV array fed water pumping system employing zeta converter", IEEE 6th India International Conference on Power Electronics. (IICPE), pp. 1-6, 2014
5. Mohammed Rasheed, Rosli Omar and Marizan Sulaiman, "Design and Development of DC-DC Boost Converter based on DSP TMS320F2812 for PV Application" Indian Journal of Science and Technology, Vol.9, no.44, Nov 2016.
6. T.-J. Liang, J.-H. Lee, "Double-deck buck-boost converter with soft switching operation", *IEEE Trans. Power. Electron.*, vol. 31, no. 6, pp. 4324-4330, Jun. 2016.
7. Xiong, Song, Siew-Chong Tan, and Siu-Chung Wong. "Analysis and design of a high-voltage-gain hybrid switched-capacitor buck converter", IEEE Trans on Circuits and Systems I: Regular Papers, vol.59, no.5, pp.1132-1141, May 2012
8. W. Khadmun, W. Subsinghaa, High Voltage Gain Interleaved DC Boost Converter Application for Photovoltaic Generation System, Elsevier Energy Procedia Journal, 2013; 34: 390 – 398.
9. A. Fardoun, E. H. Ismail, A. J. Sabzali, M. A. Al-Saffar, "New Efficient Bridgeless Cuk Rectifiers for PFC Applications," Power Electronics, IEEE Transactions on , vol.27, no.7, pp.3292-3301, July 2012.
10. J.-W. Yang and H.-L. Do, "Bridgeless SEPIC Converter With a Ripple-Free Input Current," *IEEE Trans. Power Electron.*, vol. 28, no. 7, pp. 3388–3394, Jul. 2013.
11. S.Jain, A.K.Thopukara, R. Karampuri, and V.T. Somasekhar, "A Single- Stage Photovoltaic System for a Dual-Inverter-Fed Open-End Winding Induction Motor Drive for Pumping Applications," *IEEE Transactions on Power Electronics,* , vol.30, no.9, pp.4809-4818, Sept. 2015.
12. G.J.Kish, J.J. Lee and P.W. Lehn, "Modelling and control of photovoltaic panels utilising the incremental conductance method for maximum power point tracking," *IET Renewable Power Generation*, vol.6, no.4, pp.259- 266, July 2012.
13. Terki, A., Moussi, A., Betka, A., et al.: 'An improved efficiency of fuzzy logic control of PMBLDC for PV pumping system', Appl. Math. Model, 2012, 36, (3), pp. 934–944
14. De Brito, M.A.G., Galotto, L., Sampaio, L.P., et al.: 'Evaluation of the main MPPT techniques for photovoltaic applications', IEEE Trans. Ind. Electron., 2013, 60, (3), pp. 1156–1167
15. Park, Ki-Bum, Gun-Woo Moon, and Myung-Joong Youn. "Nonisolated high step-up stacked converter based on boost-integrated isolated converter", IEEE Trans on Power Electronics, vol.26, no.2, pp.577-587, Feb 2012.
16. A. Xia, Y. Xiao, W. Chen, T. Shi, "Torque ripple reduction in brushless dc drives based on reference current optimization using integral variable structure control", IEEE Transactions on Industrial Electronics, vol. 61, no. 2, pp. 738-752, Feb. 2014.
17. J. Shi, T. Li, "New method to eliminate commutation torque ripple of brushless DC motor with minimum commutation time", *IEEE Transactions on Industrial Electronics*, vol. 60, no. 6, pp. 2139-2146, 2013.
18. G. Feng, C. Lai, N. C. Kar, "A closed-loop fuzzy-logic-based current controller for PMSM torque ripple minimization using the magnitude of speed harmonic as the feedback control signal", *IEEE Transactions on Industrial Electronics*, vol. 64, no. 4, pp. 2642-2653, April 2017.
19. A. Terki, A. Moussi, A. Betka, and N. Terki, "An improved efficiency of fuzzy logic control of PMBLDC for PV pumping system," *Appl. Math. Modell.*, vol. 36, no. 3, pp. 934–944, Mar. 2012.
20. A. Mohamed S Zaky, Mohamed K. Metwaly, " A Performance Investigation of a Four Switch Three Phase Inverter Fed IM drives at Low Speeds Using Fuzzy Logic & PI Controllers" IEEE Transactions on Power Electronics., Vol. 32, no.5, May 2017.
21. M. Singh and A. Chandra, "Real-time implementation of ANFIS control for renewable interfacing inverter in 3P4W distribution network", IEEE Trans. Ind. Electron., vol. 60, no. 1, pp. 121-128, 2013.
22. L. S. Yang, T. J. Liang, "Analysis and implementation of a novel bidirectional DC-DC converter", *IEEE Trans. Ind. Electron.*, vol. 59, no. 1, pp. 422-434, Jan. 2012.